International Journal of Heat and Technology
Vol. 41, No. 5, October, 2023, pp. 1264-1272
Journal homepage: http://iieta.org/journals/ijht

Examining the Influence of Thermal Stress on the Seismic Resilience of Prefabricated Box Culverts

Hua Wang[1], Xuetao Zhao[1], Yixiang Deng[2*]

[1] Henan Transport Investment Shensui Expressway Co., Ltd., Zhengzhou 450018, China
[2] School of Civil Engineering, Xuchang University, Xuchang 461000, China

Corresponding Author Email: 20192002@xcu.edu.cn

https://doi.org/10.18280/ijht.410516

Received: 2 June 2023
Revised: 9 September 2023
Accepted: 16 September 2023
Available online: 31 October 2023

Keywords:
prefabricated box culverts, elevated temperature, thermal stress-strain relationship, dynamical constitutive model, seismic resilience

ABSTRACT

In the realm of large-scale underground transportation engineering, prefabricated box culverts have emerged as a predominant structural element. However, their performance is potentially compromised under the duress of high temperatures, prevalent during natural or man-made disasters such as earthquakes and fires. Prior investigations predominantly focus on the performance analysis of these structures at ambient temperatures, leaving their behavior under elevated temperatures relatively unexplored. This gap in research is addressed in this study, wherein the thermal stress-strain relationship of prefabricated box culverts under high-temperature conditions is meticulously examined. A dynamical constitutive model for these structures at elevated temperatures is also proposed, paving the way for a comprehensive analysis of their seismic resilience. The insights gleaned from this study not only furnish theoretical guidance for the design and construction of prefabricated box culverts but also establish a foundational framework for subsequent inquiries in this domain.

1. INTRODUCTION

The advent of rapid global economic progression has been accompanied by an expansive growth in large-scale infrastructure, leading to an extensive application of prefabricated box culverts in diverse underground traffic engineering projects [1-4]. These structures, subjected to high temperatures resulting from natural and man-made phenomena such as earthquakes and fires, may experience alterations in structural performance [5, 6]. It is of high importance, therefore, that the behavior of prefabricated box culverts under conditions of elevated temperature is thoroughly investigated [7-10].

The exploration of seismic resilience of prefabricated box culverts is instrumental as it not only provides a scientific foundation for both design and construction, but also facilitates the effective prediction and assessment of safety and reliability under specified conditions [11, 12]. It is acknowledged that thermal stress, particularly at elevated temperatures, holds the potential to significantly influence the performance of these structures, a factor that becomes increasingly critical under extreme conditions such as seismic events [13]. Therefore, a comprehensive understanding of how thermal stress impacts the seismic behavior of prefabricated box culverts, especially when subjected to elevated temperatures, is deemed imperative for the assurance of both public safety and engineering integrity.

The predominant focus of extant research methodologies has been placed upon the analysis of prefabricated box culverts under ambient temperature conditions, leaving the phenomena under elevated temperature states somewhat underexplored. Additionally, it has been observed that prior investigations into thermal stress within prefabricated box culverts have typically been constrained to singular loading conditions [14-16], thereby overlooking the intricate loading scenarios that may manifest in practical engineering endeavors, such as cyclic loading. Consequently, this has culminated in a partial comprehension of the seismic resilience of prefabricated box culverts when subjected to extreme conditions [17-19].

This text primarily revolves around two core topics: firstly, the thermal stress-strain relationship of prefabricated box culverts under elevated temperature conditions is analyzed; secondly, the seismic performance of prefabricated box culverts at elevated temperatures is investigated, with the establishment of a corresponding dynamical constitutive model and further dynamic time-history analysis conducted. Through this series of studies, the text not only provides robust theoretical support for the design, construction, and evaluation of prefabricated box culverts but also offers new perspectives and methodologies for research in related fields, holding significant academic and engineering application value.

2. THERMAL STRESS-STRAIN RELATIONSHIPS OF PREFABRICATED BOX CULVERTS UNDER ELEVATED TEMPERATURE CONDITIONS

Box culverts, predominantly constructed from concrete and steel, exhibit significant disparities in thermal properties when subjected to elevated temperatures. Under such conditions, concrete is prone to thermal cracking, moisture depletion, and a diminution in strength, while steel may experience yielding and a decline in its strength. The elucidation of thermal stress-strain relationships of these materials at elevated temperatures is crucial for the prediction and assessment of box culvert behavior in scenarios such as fires or other high-temperature

events.

The design of prefabricated box culverts necessitates the utilization of various concrete materials, each selected for specific functions and locations. Concrete Filled Steel Tube (CFST), a composite material harnessing the advantages of both steel and concrete, is recognized for its exceptional load-bearing capacity and ductility. Consequently, it is usually utilized in the primary load-bearing elements of prefabricated box culverts, such as columns and main beams. Conversely, conventional concrete is typically employed for the culvert's top and bottom sections, where stress distribution is relatively uniform, mitigating the necessity for materials with heightened strength and ductility. This study focuses on the analysis of thermal stress-strain relationships of both CFST and conventional concrete within prefabricated box culverts under conditions of elevated temperature.

In compressive states, the thermal stress-strain relationship of CFST is initially linear at lower stress levels, attributed to the collaborative load-bearing of both concrete and steel tube. As temperatures escalate, the evaporation of internal moisture in the concrete can result in micro-structural cracks and a potential precipitous decline in load-bearing capacity beyond certain strain levels. Subsequent to the failure of concrete, the load is primarily borne by the steel tube. Nonetheless, a further temperature increase leads to a reduction in the steel's yield strength, implying a diminished yield stress for the CFST at elevated temperatures. Post-yielding of the steel tube, a phase of hardening and subsequent softening is observed, paralleling the thermal stress-strain behavior of steel.

Under high-temperature conditions, the protective efficacy of concrete on the steel tube may be compromised, potentially resulting in local buckling of the steel tube, particularly under conditions of high stress and temperature. The synergistic effects of concrete and steel may be compromised at elevated temperatures, owing to alterations in the properties of both materials. As a result, the cumulative load-bearing capacity of CFST may not equate to the sum of the individual load-bearing capacities of concrete and steel. At extreme strains and temperatures, CFST is susceptible to fracturing, a phenomenon attributable to the disintegration of concrete and the rupture of steel. Assuming the maximal temperature is represented by Y_{MAX}, then the stress-strain relationship model of CFST can be written as follows:

$$
\begin{aligned}
&t=\begin{cases}2z-z^2,(z\le 1)\\ \dfrac{z}{\alpha_p(z-1)^{\lambda}+z}\end{cases}\\
&where: z=\frac{\gamma}{\gamma_{v0}}, t=\frac{\delta}{\delta_{v0}},\\
&\delta_{v0}=d_v'/\left[1+2.4(Y_{MAX}-20)\cdot 10^{-17}\right]\\
&\gamma_0=\gamma_v+800z^{0.2}\cdot 10^{-16};\gamma_v\\
&=(1300+12.5d_v')\cdot 10^{-6}\cdot\left[1+\left(1500Y_{MAX}+5Y_{MAX}^2\right)\cdot 10^6\right]
\end{aligned}
\tag{1}
$$

In conditions of compression and at lower stress levels, conventional concrete is observed to demonstrate linear elastic behavior within its thermal stress-strain relationship. This phenomenon can be attributed to the preservation of the material's micro-structure during this initial phase. Upon reaching temperatures in the vicinity of 100℃, the evaporation of capillary water within the concrete commences, potentially resulting in augmented internal pressure and the inception of micro-cracks. As exposure to elevated temperatures is sustained, a discernible decline in the compressive strength of the concrete is noted, accompanied by a possible increment in strain. These alterations are ascribed to a series of micro-structural transformations, including chemical dehydration and the decomposition of limestone. Subsequent to these events, the thermal stress-strain behavior of the concrete transitions into a pronounced nonlinear regime, characterized by an expedited reduction in strength and an increase in strain rate. Thermal expansion of the material is manifested at elevated temperatures, which may induce additional stresses when external constraints are present. Continued thermal elevation exacerbates the degradation of the concrete, potentially leading to transformations in mineral components such as quartz. Prolonged thermal exposure also raises the possibility of concrete carbonation, further compromising the material's structural integrity. In scenarios involving extreme temperatures and strains, the concrete is susceptible to fragmentation, primarily due to the destabilization of its internal micro-structure. For the purpose of mathematical representation, let $d_{vi,Yl}$ denote the cube compressive strength of the concrete subsequent to high-temperature exposure, and d_{vi} represent its cube compressive strength at ambient temperature, then he high-temperature degradation model of conventional concrete is thus expressed as follows:

$$
\begin{aligned}
&d_{vi,Yl}=d_{vi} \qquad 0°C\le Y_{MAX}\le 200°C\\
&d_{vi,Yl}=d_{vi}\cdot\left[0.0015\cdot(200-Y_{MAX})+1\right]\\
&\qquad 200°V<Y_{MAX}\le 500°C\\
&d_{vi,Yl}=d_{vi}\cdot\left[0.003\cdot(600-Y_{MAX})+0.25\right]\\
&\qquad 500°V<Y_{MAX}\le 600°C\\
&d_{vi,Yl}=d_{vi}\cdot\left[7.5\times 10^{-4}\cdot(200-Y_{MAX})+0.25\right]\\
&\qquad 600°V<Y_{MAX}\le 800°C
\end{aligned}
\tag{2}
$$

Additionally, let γ_0 and δ_0 respectively denote the peak strain and stress of the concrete at room temperature, while $\gamma_{0,Yl}$ and $\delta_{0,Yl}$ represent the peak strain and stress after exposure to high temperatures. The stress-strain relationship model under these conditions is provided by the subsequent expressions:

$$
\begin{aligned}
&t=0.63z+1.74z^2-1.37z^3 \qquad z\le 1\\
&t=\left(0.67z-0.22z^2\right)/\left(1-1.33z+0.78z^2\right) \qquad z>1\\
&where: z=\gamma/\gamma_{0,Yl}, t=\delta/\delta_{0,Yl}\\
&\gamma_{0,Yl}/\gamma_0=1 \qquad Y_{MAX}\le 200°C\\
&\gamma_{0,Yl}/\gamma_0=0.58+2.35\cdot(Y_{MAX}-20)/1000\\
&\qquad Y_{MAX}>200°C\\
&\gamma_{0,Yl}/\gamma_0=1-0.58\cdot(Y_{MAX}-20)/1000\\
&\qquad Y_{MAX}\le 200°C\\
&\delta_{0,Yl}/\sigma_0=1.15-1.39\cdot(Y_{MAX}-20)/1000\\
&\qquad Y_{MAX}>200°C
\end{aligned}
\tag{3}
$$

Under conditions of compression and lower stress, CFST exhibits a thermal stress-strain relationship characteristic of linear elastic behavior. The dual burden of tensile stress is shared between the concrete and steel tube at this juncture. Given the markedly lower tensile strength of concrete relative to its compressive counterpart, micro-cracks in the concrete are prone to initiate at relatively minor strains. The propensity

for cracking is exacerbated by elevated temperatures, as the concurrent phenomena of water evaporation and thermal expansion amplify internal stresses. Upon the formation of cracks in the concrete, the onus of load-bearing shifts predominantly to the steel tube, rendering the thermal stress-strain relationship predominantly contingent on the steel's properties. A rise in temperature precipitates a gradual diminution of the steel's elastic modulus, culminating in increased strains and a concomitant reduction in yield strength. Notwithstanding, the steel's comparatively superior tensile strength ensures that the yield stress of the CFST remains relatively robust under tensile conditions. High temperatures induce thermal expansion, potentially engendering additional stresses, especially when external constraints are imposed. Escalating temperatures may further compromise the synergistic interaction between concrete and steel, a deterioration exacerbated post-cracking of the concrete. Although steel retains a degree of ductility at elevated temperatures, it is acknowledged that this property diminishes with increasing temperature. In extreme scenarios of high strains and temperatures, the steel tube is susceptible to fracture, culminating in the structural failure of the CFST.

Conversely, conventional concrete, under compressive conditions and lower stress levels, tends to manifest a linear elastic behavior in its thermal stress-strain relationship, attributed to the preservation of its micro-structure. When temperatures approach 100°C, the evaporation of capillary water within the concrete is initiated, potentially escalating internal stresses and fostering the development of micro-cracks, thereby diminishing the concrete's capacity to bear tensile loads. The inherently low tensile strength of concrete is further compromised at elevated temperatures. As stresses intensify, the concrete is observed to exhibit a pronounced nonlinear increase in strain, which may eventually culminate in the formation of macro-cracks. High-temperature conditions facilitate the expansion and coalescence of these cracks, precipitating a significant reduction in cross-sectional area and, by extension, load-bearing capacity. Thermal expansion at elevated temperatures may exacerbate internal stresses, particularly under constrained conditions. Transformations in mineral components such as quartz, induced by high temperatures, contribute to structural degradation and further strength reduction. Under conditions of thermal cycling, the concrete may exhibit symptoms of thermal fatigue, manifesting as a progressive increase in strain under constant stress levels. In scenarios of protracted tensile stress and high-temperature exposure, the concrete is vulnerable to sudden failure, evidenced by rapid crack propagation and fracture. The following expression encapsulates the relationship model between the tensile strength of concrete post high-temperature exposure and the maximum fire temperature:

$$d_{yo}\left(Y_{MAX}\right)=0.98+\begin{bmatrix}1.56\cdot\left(Y_{MAX}/100\right)-4.35\cdot\left(Y_{MAX}/100\right)^{2}\\+0.34\left(Y_{MAX}/100\right)^{3}\end{bmatrix}\cdot 100^{-2}\cdot d_{y} \quad (4)$$

Let $\gamma_{CR}(Y_{MAX})=d_{yo}(Y_{MAX})/R_{vo}(Y_{MAX})$, and the post-high-temperature elastic modulus of concrete represented by $R_{vo}(Y_{MAX})$, then the limit tensile strain calculated by the following equation:

$$\gamma_{TU}\left(Y_{MAX}\right)=15\gamma_{CR}\left(Y_{MAX}\right) \quad (5)$$

Under conditions of elevated temperatures, certain characteristics are exhibited by the tensile thermo-stress-strain relationship of steel in prefabricated box culverts. In the regime of lower stress, the steel's thermo-stress-strain relationship is characterized by linear elastic behavior, a phenomenon attributed to the maintenance of the steel's micro-structural integrity within this specific stress range. As a function of increasing temperature, a reduction in the steel's elastic modulus is observed, leading to increased strain under a constant stress condition. Concurrently, a diminution in the steel's yield strength is noted, indicative of a potential onset of yielding at reduced stress levels. Despite this observed reduction in yield strength under elevated temperatures, the steel is found to maintain its strain hardening behavior subsequent to yielding, a phenomenon that may be expedited under conditions of elevated temperature. Like most materials, the steel in question is subject to thermal expansion when subjected to heating, a process that has the potential to induce additional internal stresses, especially under conditions of constraint. Extended exposure to both tensile stress and high temperatures is linked to the manifestation of creep, a phenomenon characterized by a time-dependent increase in strain, even under conditions of constant stress. At specific temperature thresholds, micro-structural alterations in the steel, such as phase transformations, may transpire, exerting further influence on its mechanical properties. The steel's susceptibility to oxidation or corrosion, contingent on the prevailing environmental conditions and temperatures, may precipitate changes in both surface and internal mechanical properties. In scenarios characterized by extremely high strains and temperatures, areas of the steel with pre-existing flaws or damage may be predisposed to fracturing.

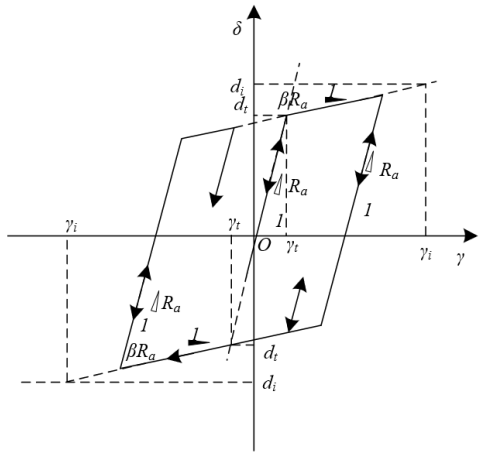

Figure 1. Stress-strain relationship of steel material in prefabricated box culvert

In instances of exposure to high temperatures, a transient reduction in the steel's elastic modulus is often recorded, with the potential for partial or complete restoration of its original value during the cooling phase, particularly under conditions of gradual cooling. Conversely, rapid cooling has the potential to precipitate swift alterations in the steel's micro-structure, implications of which extend to the recovery trajectory of its elastic modulus. Prolonged exposure to elevated temperatures is correlated with a reduction in yield strength, whereas specific micro-structural changes during the cooling phase, such as recrystallization or solid solution treatment, may contribute to an augmentation in yield strength. It is

noteworthy, however, that an excessively rapid cooling rate may lead to the formation of a hard and brittle Martensite Phase, resulting in an enhanced yield strength but compromised toughness. The stress-strain relationship of steel in prefabricated box culverts, post exposure to high temperatures, is depicted in Figure 1.

Assuming $d_t(Y_{MAX})$ represents the yield strength at the maximum temperature Y, then the stress-strain relationship of the steel after high-temperature natural cooling is:

$$\delta = \begin{cases} R_a\left(Y_{MAX}\right), \gamma < \gamma_t\left(Y_{MAX}\right) \\ d_t\left(Y_{MAX}\right) + R_a\left(Y_{MAX}\right)\left[\gamma - \gamma_t\left(Y_{MAX}\right)\right], \\ \gamma > \gamma_t\left(Y_{MAX}\right) \end{cases} \tag{6}$$

And $d_t(Y_{MAX})$ can be calculated using the following equation:

$$\frac{d_t\left(Y_{MAX}\right)}{d_t} = \begin{cases} 1.0, \left(Y_{MAX} \le 500\right) \\ 1 - 5.82\times10^{-4}\left(Y_{MAX} - 500\right), \left(Y_{MAX} > 500\right) \end{cases} \tag{7}$$

Assuming $R_a(Y_{MAX})$ represents the elastic modulus of the steel during the elastic phase, then the elastic modulus of the steel post-high-temperature cooling can be calculated using the subsequent equation:

$$\frac{R_a\left(Y_{\max}\right)}{R_a} = \begin{cases} 1.0, \left(Y_{\max} \le 500\right) \\ 1 - 1.30\times10^{-4}\left(Y_{\max} - 500\right), \left(Y_{\max} > 500\right) \end{cases} \tag{8}$$

The elastic modulus during the strengthening phase can be determined through the subsequent equation:

$$R_a\left(Y_{MAX}\right) = 0.01R_a\left(Y_{MAX}\right) \tag{9}$$

3. SEISMIC PERFORMANCE OF PREFABRICATED BOX CULVERT UNDER HIGH-TEMPERATURE CONDITIONS

3.1 Dynamic constitutive model of prefabricated box culvert under high-temperature conditions

Figure 2 is delineated to demonstrate the interactions occurring between the soil and the prefabricated box culvert structure. As can be known from the figure, building a plastic loss model for analyzing the various loads of soil and the prefabricated box culvert and determining parameters required by the model are of important significance for both scholarly inquiry and practical engineering scenarios. Common linear elastic models are found wanting in their capacity to faithfully predict the response characteristics of prefabricated box culvert concrete under complex loading conditions, especially in regions experiencing substantial deformation and plasticity. The material under scrutiny, the concrete of the prefabricated box culvert, is observed to manifest pronounced nonlinear behavior when subjected to substantial or recurrent loads. Enhancement in prediction accuracy is achieved through the introduction of a damage factor, rooted in both plastic and inelastic strain.

In this study, six input parameters have been discerned. Under compressive conditions, these parameters are δ_v, $\gamma^{\sim IN}{}_v$, and f_v, while under tensile conditions, they are δ_y, $\gamma^{\sim IN}{}_y$, and f_y. Compression and tension induced stresses in the concrete under dynamic loading are symbolized by δ_v and δ_y, respectively. In a similar vein, $\gamma^{\sim IN}{}_v$ and $\gamma^{\sim IN}{}_y$ symbolize the inelastic compressive and tensile strains, serving as input for the plastic damage model. Damage factors corresponding to the material's behavior under compressive and tensile states are represented by f_v and $_tf_y$, respectively.

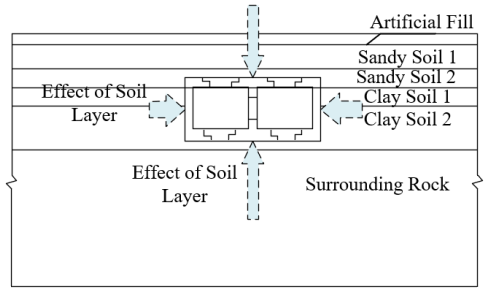

Figure 2. Interactions between soil and the prefabricated box culvert structure

The stress-strain relationship of the concrete under compressive and tensile conditions post high-temperature exposure is postulated to be δ_v-γ_v and δ_y-γ_y, respectively. The undisturbed elastic moduli of the concrete, following high-temperature exposure and under compressive and tensile states, are designated as R_{v0} and R_{y0}, respectively. The inelastic strains, $\gamma^{\sim IN}{}_v$ and $\gamma^{\sim IN}{}_y$, are derivable through following equations:

$$\begin{cases} \tilde{\gamma}_v^{IN} = \gamma_v - \tilde{\gamma}_v^{rm} = \gamma_v - \dfrac{\delta_v}{R_{v0}} \\ \tilde{\gamma}_y^{IN} = \gamma_y - \tilde{\gamma}_y^{rm} = \gamma_y - \dfrac{\delta_y}{R_{y0}} \end{cases} \tag{10}$$

Introducing proportional coefficients between plastic strains ($\gamma^{\sim PL}{}_v$, $\gamma^{\sim PL}{}_y$) and inelastic strains ($\gamma^{\sim IN}{}_v$, $\gamma^{\sim IN}{}_y$), yields n_v=$\gamma^{\sim PL}{}_v/\gamma^{\sim IN}{}_v$ and n_y=$\gamma^{\sim PL}{}_y/\gamma^{\sim IN}{}_y$. With subscripts v and y denoting the stress states of compression and tension in the concrete, the equation below is provided for the computation of the damage factor:

$$f_{v(y)} = 1 - \frac{\delta_{v(y)}R_{v(y)0}^{-1}}{\tilde{\gamma}_{v(y)}^{PL}\left(1/n_{v(y)} - 1\right) + \delta_{v(y)}R_{v(y)0}^{-1}} \tag{11}$$

3.2 Dynamic time-history analysis of prefabricated box culvert under high-temperature conditions

Distinctive stress and deformation characteristics are exhibited by the structure of prefabricated box culverts under various seismic magnitudes (minor, moderate, or major earthquakes). During minor earthquakes, the components of the prefabricated box culvert structure primarily remain in an elastic working state, with negligible apparent damage. In contrast, moderate to major earthquakes induce increased stress and deformation, potentially leading to various phenomena ranging from minute cracks to severe damage. Particular attention should be paid to the stress and deformation at the connections, as these represent the vulnerable links in the prefabricated structure.

Under the influence of major earthquakes, the prefabricated box culvert structure may demonstrate pronounced nonlinear

behavior, including plastic deformation, crack propagation, and damage at the joints. The elasto-plastic time-history analysis method is capable of capturing these nonlinear responses, providing engineers with a more accurate prediction of the structural performance. In this study, the elasto-plastic time-history analysis method is employed to offer precise predictions for the response of the prefabricated box culvert structure under consecutive or multiple earthquake excitations. It is posited that the nodal displacement vector is denoted as i, while the mass, damping, and stiffness matrices of the structure are represented by L, V, and J, respectively. External forces are denoted by D, time by y, and ground motion acceleration by $\ddot{i}_h$. Given that the earthquake effect can be expressed as $D = -L\ddot{i}_h$, the theoretical formula for the elasto-plastic time-history analysis adopted in this study is given by the following equation:

$$L\ddot{i} + V\dot{i} + Ji = D(y) \tag{12}$$

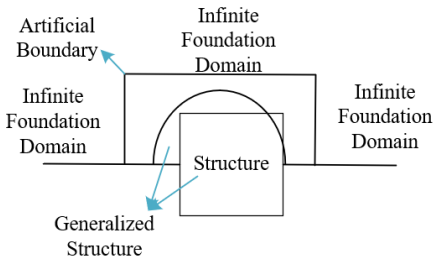

Figure 3. Artificial boundary of prefabricated box culvert structure

In Figure 3, a schematic representation of the artificial boundary of a prefabricated box culvert structure is presented. Due to internal friction within materials and other nonlinear factors, energy is dissipated during the vibrations experienced by actual structures. Compared to other complex damping models, the proportional viscous damping model boasts a simpler mathematical form. This simplicity facilitates implementation within computer programs, enhancing computational efficiency while ensuring accuracy. In this study, the proportional viscous damping model has been selected for analyzing the dynamic response of the components of the prefabricated box culvert structure. This selection aims to simulate the effect of energy dissipation, providing a more realistic prediction of dynamic response. The proportional coefficients within the model are denoted by β and α, and are calculated based on the natural frequency of the structure:

$$[V] = \beta[L] + \alpha[J] \tag{13}$$

3.3 Seismic performance indicators and structural failure criteria

In this section, seismic safety evaluation indicators for prefabricated box culvert structure components are enumerated from two aspects: structural and performance displacement responses. Structural displacement responses encompass: a) Maximum Top Displacement: The overall deformation extent of the structure under seismic impact is directly reflected by the displacement magnitude at the structure's top. b) Relative Displacement: The evaluation of relative displacements between various floor slabs can be utilized to assess the shear deformation of the structure. Should the relative displacement at any level surpass the stipulated limit, potential structural damage or failure may ensue. c) Displacement Angle: The overall deformation and tilt of the structure are indicated by the displacement angle, defined as the ratio of the displacement difference between the lowest and highest points of the structure to its height. Exceedance of a certain threshold may impact the overall stability of the structure. d) Residual Displacement: Post-seismic activity, the structure may exhibit certain residual displacements, predominantly due to plastic deformation. High residual displacements may necessitate structural repair or impede its usability.

Performance displacement responses include: a) Inter-story Drift: By evaluating the displacement differences between stories, insights into the shear deformation of the structure during an earthquake can be gained. It serves as a crucial index for assessing whether the structure has entered a nonlinear state and the potential extent of damage. b) Displacement Demand-to-Capacity Ratio: The seismic safety margin of the structure is assessed by comparing the actual displacement demand during an earthquake to its displacement capacity. Exceedance of capacity by demand could result in structural damage. c) Performance Point Displacement: Based on the structure's shear displacement curve, its performance point displacement can be determined. This displacement can then be compared to a predetermined performance target displacement to assess whether the structure meets the set performance objectives. d) Formation and Development of Plastic Hinges: The formation and development of plastic hinges at critical structural locations, such as columns, beams, and connections, serve as a significant indicator for evaluating the seismic performance of the structure.

Special attention needs to be given to the failure criteria of prefabricated box culvert structure components subjected to earthquake forces following exposure to high temperatures, as their structural performance may have been compromised. Stress failure may occur if, post high-temperature exposure, the strength of concrete, steel reinforcement, and steel materials has likely diminished. Structural components may fail if the actual stress exceeds the yield or ultimate strength of the materials post high-temperature exposure. Displacement failure is of particular concern for prefabricated structures, where joints and connections are critical. Joints or connections may be compromised if the structure's maximum displacement during an earthquake exceeds the maximum allowable design displacement. Figure 4 presents the load-displacement curve of the prefabricated box culvert structure components.

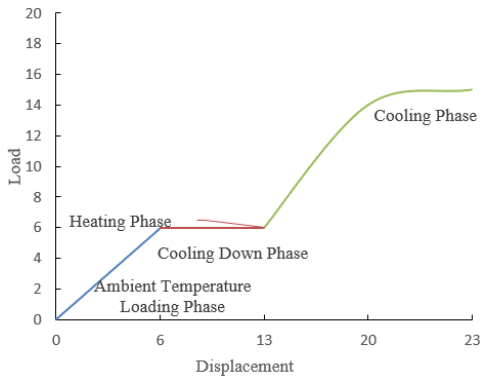

Figure 4. Load-displacement curve of prefabricated box culvert structure components

Let Δi_r denote the maximum inter-story displacement of a structure subjected to a frequent earthquake, $[\phi_r]$ denote the allowable value of inter-story drift, and g denote the standard height of a story. The verification formula for inter-story drift is given by the following equation:

$$\Delta i_r \leq [\phi_r] g \tag{14}$$

4. EXPERIMENTAL RESULTS AND ANALYSIS

At first, this study discussed the thermal stress-strain relationship of prefabricated box culverts under high-temperature conditions. The two figures provided above display the maximum acceleration of the CFST and the ordinary concrete in the prefabricated box culvert during the transition from high temperatures to cooling. Several observations were made from the data presented in the figures. It is observed that the maximum acceleration at all measurement points of the CFST is consistently higher than that of the ordinary concrete. At a constant temperature, there is a noticeable difference in maximum acceleration between components of different specifications or strength grades. It can be concluded that the concrete and steel may experience a decrease in strength and thermal expansion under high temperatures. These changes might lead to variations in the dynamic response of the materials, as indicated by the data, where an increase in temperature correlates with an increase in maximum acceleration. This phenomenon is potentially related to changes in material properties and thermal expansion. It is evident from the figures that the maximum acceleration of the CFST is generally higher than that of the ordinary concrete. This disparity could be attributed to the internal steel tube of the CFST, which endows it with superior load-bearing capacity and rigidity. Consequently, under the same dynamic load, the acceleration experienced is greater. Materials of different specifications or strength grades might exhibit varying performance and responses, as reflected in the maximum acceleration of components with different specifications presented in the Figure 5.

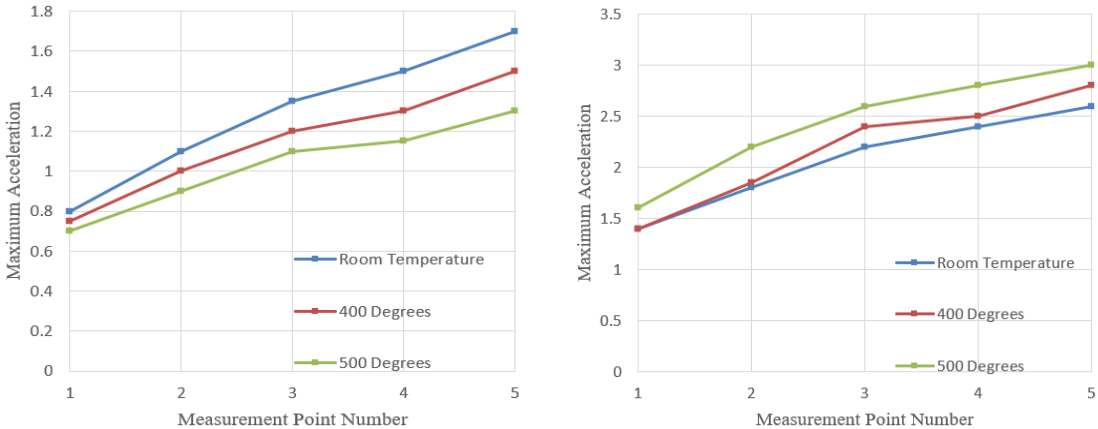

Figure 5. Maximum acceleration of prefabricated box culvert concrete during the high-temperature to cooling process

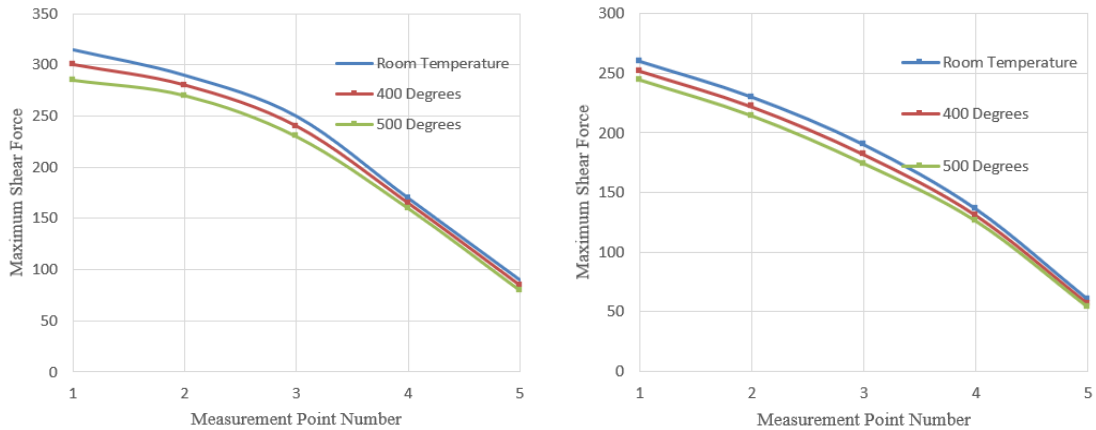

Figure 6. Maximum shear force of prefabricated box culvert concrete during the high-temperature to cooling process

From Figure 6, it is observed that both the CFST and the ordinary concrete exhibit a decreasing trend in their maximum shear force. This trend correlates with the previously discussed changes in material properties under high-temperature conditions; elevated temperatures may lead to a degradation in some mechanical properties of concrete and steel, resulting in a reduced shear resistance when subjected to external forces. Across all considered temperature ranges, the maximum shear force of the CFST consistently surpasses that of the regular concrete. This can be attributed to the composite structure of CFST, which combines concrete with steel, enhancing its shear resistance. Additionally, the introduction of steel may increase the structural ductility, slowing down the rate of performance degradation under high temperatures. The three

curves—representing room temperature, 400 degrees, and 500 degrees—depict different high-temperature treatment scenarios. It is evident from the figure that the trend of decreasing maximum shear force becomes more pronounced with increasing temperature, indicating that higher temperatures exert a further detrimental impact on the shear resistance of the concrete. Therefore, it can be concluded that during the process from high temperature to cooling, the maximum shear force of both the CFST and ordinary concrete in the prefabricated box culvert decreases, with the CFST consistently exhibiting superior shear resistance. Furthermore, the higher the temperature during high-temperature treatment, the more pronounced the reduction trend. This underscores the importance of considering the impact of temperature on the performance of prefabricated box culvert structures in their design.

Table 1. Comparison of the dynamic characteristics of the prefabricated box culvert structure

Mode Order	Reference Vibration Period	Simulated Vibration Period	Simulated/Reference Vibration Period Ratio
1	1.895	1.784	0.951
2	1.357	0.324	0.942
3	0.784	0.784	0.983
4	0.532	0.517	0.941
5	0.461	0.475	1.024
6	0.328	0.312	0.975

In this study, a dynamical constitutive model of the prefabricated box culvert under high temperatures was established and its seismic performance was analyzed. By examining the "Simulated/Reference Vibration Period Ratio" column, it is observed that the simulated vibration periods across all modes are remarkably close to the reference vibration periods. The majority of the ratios lie between 0.9 and 1.1, indicating that the results of the simulation are relatively accurate and in good agreement with actual conditions. As can be seen from the Table 1, both the reference vibration period and the simulated vibration period exhibit a declining trend as the mode order increases. This trend is in accordance with the fundamental principles of structural dynamics, where higher modes correspond to higher frequency vibrations, resulting in shorter vibration periods. Previous discussions have established that the mechanical properties of the prefabricated box culvert deteriorate in high-temperature environments, potentially affecting its dynamic performance and altering the vibration periods. Despite certain discrepancies between the simulated and reference vibration periods, as indicated in the Table 1, these discrepancies are not substantial. This suggests that the impact of high-temperature environments does not induce drastic changes in the seismic performance of the structure. In conclusion, the simulated vibration periods of the prefabricated box culvert structure in high-temperature environments are relatively close to the reference vibration periods, with minor differences. This implies that the dynamic characteristics of the structure may not be severely affected by high-temperature environments. However, it is crucial to take into consideration other factors, such as changes in material properties and stress distribution under high temperatures, to ensure the structural safety in practical applications.

In Figure 7(a), the displacement response of the prefabricated box culvert structure at different temperatures is depicted. It is observed that, as time progresses, the displacement responses under all temperature conditions initially increase and then tend to stabilize. For the concrete at room temperature, both the rate of increase and the stable value of its displacement response are smaller than those of the concrete under the other three temperature conditions. This could be attributed to the concrete at room temperature not being affected by high temperatures, thus exhibiting more stable mechanical properties. In contrast, as the temperature rises (400 degrees, 500 degrees, 600 degrees), the peak values of the displacement response gradually increase, though the differences are not significant. Figure 7(b) illustrates the variation of the displacement response of the prefabricated box culvert structure over time under different temperature conditions. A strong vibration response is manifested under all temperature conditions. It is noticeable that the responses under all temperature conditions display a similar oscillatory pattern, yet the amplitude of fluctuation for the concrete at room temperature is relatively smaller, consistent with the observations made in Figure 7(a). It can be concluded that high temperatures indeed exert an influence on the displacement response of the prefabricated box culvert structure, resulting in its increase. With the escalation of temperature, the peak values of the displacement response also gradually rise. The concrete at room temperature, unaffected by high temperatures, manifests a relatively smaller displacement response, demonstrating better stability. In designing prefabricated box culvert structures under high-temperature environments, particular attention needs to be paid to their displacement responses, and measures should be considered to mitigate the additional displacement induced by high temperatures.

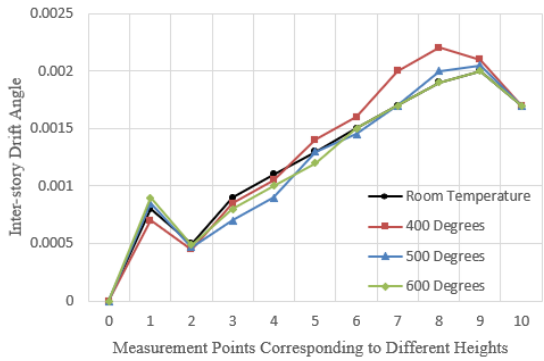

(a) Inter-story drift angle

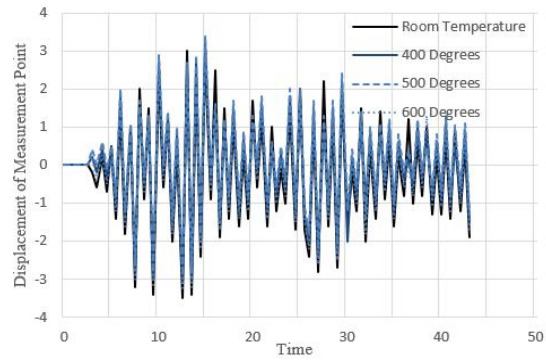

(b) Displacement of measurement point

Figure 7. Displacement response of the prefabricated box culvert structure under high temperatures

Figure 8 illustrates the variation over time of the base shear force of the prefabricated box culvert under earthquake

conditions at high temperatures. Two scenarios are considered: the concrete at room temperature and the concrete at a high temperature of 500 degrees. In both the room temperature and the 500-degree high-temperature conditions, a pronounced oscillatory pattern in base shear force is displayed, reflecting the dynamic response of the structure under seismic activity. For the concrete at room temperature, a larger amplitude of oscillation in the base shear is observed, and it remains within a relatively stable range throughout the entire observation period. In the case of the 500-degree high-temperature condition, the amplitude of oscillation in base shear force is comparatively smaller, and both the peak and trough values are slightly lower than those of the concrete at room temperature throughout the observation period. It can be concluded that the base shear force induced by seismic activity exhibits a strong oscillatory response under both conditions. The high-temperature condition (such as 500 degrees) has a noticeable impact on the base shear force of the prefabricated box culvert. Compared to the concrete at room temperature, the shear response at 500 degrees is reduced. This may imply that the structural performance of concrete under seismic activity may be compromised at high temperatures. When designing prefabricated box culvert structures, in addition to conventional seismic loads, the impact of temperature should also be taken into consideration, especially in potential high-temperature environments. Ensuring the stability and safety of the structure under these extreme conditions is of high importance.

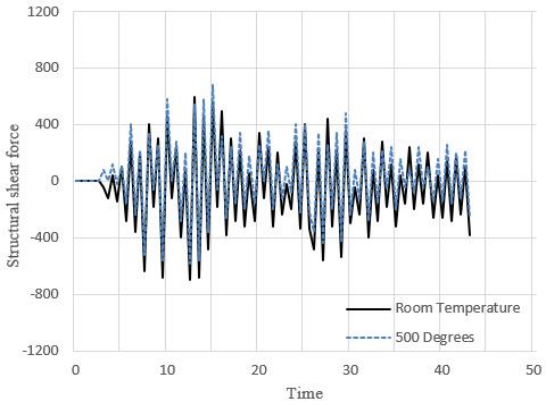

Figure 8. Base shear force of the prefabricated box culvert under earthquake conditions at high temperatures

5. CONCLUSION

An in-depth investigation into the prefabricated box culvert under high-temperature conditions has been conducted. The thermal stress-strain relationship of the prefabricated box culvert under high temperatures has been thoroughly explored. In addition, a dynamic constitutive model of the prefabricated box culvert under high temperatures has been established, and its seismic performance has been further analyzed. The experimental results have demonstrated that, under high-temperature conditions, both the CFST and the ordinary concrete exhibit varying degrees of stress reduction, indicating that an increase in temperature might adversely affect the mechanical properties of the materials. During the process from high temperature to cooling, the maximum shear forces of both the CFST and the ordinary concrete in the prefabricated box culvert decrease over time. Among them, the maximum shear force of the ordinary concrete shows a more significant reduction, while the differences in the CFST under various temperature conditions are relatively small. A comparison of the dynamic characteristics of the prefabricated box culvert structure reveals that the difference between the simulated vibration period and the reference vibration period is not significant, indicating a high reliability of the model. Under the influence of seismic activity, both the displacement response and the base shear force of the prefabricated box culvert exhibit oscillatory characteristics. Under high-temperature conditions, the responses of both displacement and shear force are relatively reduced, especially under the condition of 500 degrees.

The structural performance of the prefabricated box culvert is clearly affected by high-temperature conditions. Under such conditions, the stress performance of the concrete is diminished, and the dynamic response of the prefabricated box culvert under seismic activity is also influenced by temperature. Overall, the seismic performance of the prefabricated box culvert under high-temperature conditions may be relatively fragile. Therefore, when designing and constructing the prefabricated box culvert, the impact of temperature on structural performance should be fully considered, and necessary measures should be taken to ensure the safety and stability of the structure.

REFERENCES

[1] Zhang, C., Wu, Q., Wang, H., Zhou, H., Cao, S., Cai, C., Peng, X.D., Ma, H. (2021). Application of strain monitoring of box culvert structure in box culvert push construction. In 4th International Symposium on Power Electronics and Control Engineering (ISPECE 2021), Nanchang, China, 12080: 996-1000. https://doi.org/10.1117/12.2620282

[2] Lu, X., Liu, Y., Zhang, L. (2021). Research on deformation characteristics of tunnel box culvert structure under different construction loads. In IOP Conference Series: Earth and Environmental Science, 634(1): 012136. https://doi.org/10.1088/1755-1315/634/1/012136

[3] Gong, Y.F., Pang, Y.Z., Wang, B., Tan, G.J., Bi, H.P. (2021). Mechanical properties of new prefabricated box culvert structure based on road conditions in Jilin Province. Journal of Jilin University (Engineering and Technology Edition), 51(3): 917-924.

[4] Ozturk, K.F., Cakir, T., Araz, O. (2022). A comparative study to determine seismic response of the box culvert wing wall under influence of soil-structure interaction considering different ground motions. Soil Dynamics and Earthquake Engineering, 162: 107452. https://doi.org/10.1016/j.soildyn.2022.107452

[5] Shi, J.X. (2019). Design and analysis of double-hole box culvert structure based on beam element modeling. In IOP Conference Series: Earth and Environmental Science, 332(3): 032057. https://doi.org/10.1088/1755-1315/332/3/032057

[6] Luo, B., Ishikawa, T., Tokoro, T., Lai, H. (2017). Coupled thermo-hydro-mechanical analysis of freeze–thaw behavior of pavement structure over a box culvert. Transportation Research Record, 2656(1): 12-22. https://doi.org/10.3141/2656-02

[7] Liu, Z., Zhang, C. (2013). Shifting technique for a box

culvert structure in a cut-and-cover metro tunnel. Modern Tunnelling Technology, 50(3): 168-172. https://doi.org/10.3969/j.issn.1009-6582.2013.03.026

[8] Guven, A., Hassan, M., Sabir, S. (2013). Experimental investigation on discharge coefficient for a combined broad crested weir-box culvert structure. Journal of hydrology, 500: 97-103. https://doi.org/10.1016/j.jhydrol.2013.07.021

[9] He, F.D., Cui, J.P., Sui, J., Yu, Y.F. (2013). Analysis of differential settlement influence on internal force of box culvert structure. Applied Mechanics and Materials, 353: 225-228. https://doi.org/10.4028/www.scientific.net/AMM.353-356.225

[10] Philip, S., Rakendu, R., Lal, R. (2022). The impact of geofoam on the bending moment characteristics of reinforced concrete box culverts for road under bridge (RUB) design. Materials Today: Proceedings, 52: 2305-2314. https://doi.org/10.1016/j.matpr.2021.11.342

[11] Kheradi, H., Ye, B., Nishi, H., Oka, R., Zhang, F. (2017). Optimum pattern of ground improvement for enhancing seismic resistance of existing box culvert buried in soft ground. Tunnelling and Underground Space Technology, 69: 187-202. https://doi.org/10.1016/j.tust.2017.06.022

[12] Shimabata, T., Matsuo, T., Ohtomo, K., Morozumi, H., Fuse, T. (2019). Three-dimensional seismic analysis of underground reinforced concrete box culvert with L-junction. In FIB 2018 - Proceedings for the 2018 fib Congress: Better, Smarter, Stronger.

[13] Hata, M., Sato, M., Miyazawa, S. (2022). Experimental study on the application of cementless material with industrial by-products to steam-cured precast concrete products. Materials, 15(21): 7624. https://doi.org/10.3390/ma15217624

[14] Hua, L., Fujun, N., Yonghong, N., Xifeng, Y. (2014). Study on thermal regime of roadbed–culvert transition section along a high speed railway in seasonally frozen regions. Cold regions science and technology, 106: 216-231. https://doi.org/10.1016/j.coldregions.2014.07.008

[15] Nguyen, H.V., Nakarai, K., Okazaki, A., Karasawa, H., Tadokoro, Y., Tsujino, M. (2019). Applicability of a simplified estimation method to steam-cured expansive concrete. Cement and Concrete Composites, 95: 217-227. https://doi.org/10.1016/j.cemconcomp.2018.11.002

[16] Igawa, H., Eguchi, H., Kitsutaka, Y. (2018). A fundamental study for the self-healing performance of heavyweight concrete. Nippon Kenchiku Gakkai Kozokei Ronbunshu (Online), 83(748): 763-772. http://doi.org/10.3130/aijs.83.763

[17] Katona, M.G. (2010). Seismic design and analysis of buried structures with CANDE-2007. Transportation research record, 2172(1): 171-181. https://doi.org/10.3141/2172-19

[18] Katona, M.G. (2010). Seismic design and analysis of buried culverts and structures. Journal of pipeline systems engineering and practice, 1(3): 111-119. https://doi.org/10.1061/(ASCE)PS.1949-1204.0000057

[19] Wang, M.W., Iai, S., Tobita, T. (2006). Seismic performances of underground RC structures in liquefiable soils in nuclear plants. In Ground Modification and Seismic Mitigation, 387-394. https://doi.org/10.1061/40864(196)52